УЧЕНЫЕ ЗАПИСКИ КАЗАНСКОГО УНИВЕРСИТЕТА
Том 153, кн. 3 Физико-математические науки *2011*

UDK 519.63

POTENTIAL DOMINATED SCALAR-TENSOR COSMOLOGIES IN THE GENERAL RELATIVITY LIMIT

L. Järv, P. Kuusk, M. Saal

Abstract

We consider Friedmann – Lemaître – Robertson – Walker flat cosmological models in the framework of general Jordan frame scalar-tensor theories of gravity with arbitrary coupling function and potential. For the era when the cosmological energy density of the scalar potential dominates over the energy density of ordinary matter, we use a nonlinear approximation of the decoupled scalar field equation for the regime close to the so-called limit of general relativity where the local weak field constraints are satisfied. We consider the phase space of the scalar field and provide a complete classification of possible phase portraits. We give the solutions in cosmological time with a particular attention to the classes of models asymptotically approaching general relativity. The latter can be subsumed under two types: (i) exponential convergence, and (ii) damped oscillations around general relativity.

Key words: scalar-tensor cosmologies, general relativity limit, dark energy.

Introduction

Equations of the Einstein general relativity (GR) present a mathematical description of (macroscopic) space, time and matter. Their validity has been checked by experiments in the Solar System on scales of 10^{-3} to 10^{11} m and the results are consistent with the Einstein theory (within error margins) [1]. Astrophysical observations of galaxies and clusters can probe GR on scales of kpc to Mpc and observations of large scale structure can extend the scale to over 1 Gpc [2]. However, it seems that in the orders of magnitude considerably smaller (in quantum realm) and bigger (in the Universe as a whole) GR needs to be somehow modified, although the precise form of modified theories is not known. There are theories which claim to be suitable for quantum gravity as well as for cosmology, e.g. string and superstring theories [3], but in this paper we will consider modifications tailored for cosmology only.

Precise cosmological observations that could confirm or contest the validity of the Einstein theory and corresponding cosmological models in the orders of magnitude of the whole Universe have been made possible only during the last decades and their error margins are considerably larger than for Solar System experiments. Forty years ago the prevailing wisdom regarded the general relativistic closed Friedmann – Lemaître – Robertson – Walker (FLRW) model as the correct global model for the Universe [4]. It has an expanding homogeneous and isotropic three-space with finite volume without boundary. The present rate of expansion can be determined from observations (within error margins) and the Einstein equations predict that in this model the expansion is slowing down. The next task of observational cosmology was to determine the corresponding deceleration parameter. However, in 1998 two groups published their results [5, 6] which demonstrated that the expansion of the Universe is not decelerating, but has been accelerating for last few billion years. This fact has now been cross-checked by other independent observational data. The minimal modification to include this phenomenon into GR is to introduce an additional constant of nature (cosmological constant Λ) which can be accommodated in the Einstein theory as vacuum energy. The present day concordance model of our Universe is Λ-Cold-Dark-Matter (ΛCDM) which includes two types of ordinary matter (visible and dark) and the cosmological constant. But the numerical value of the latter one turns out to be extremely small ($\rho_\Lambda \simeq 10^{-47}$ GeV^4). This raises a problem of fine tuning and provokes to look also for other kinds of explanations. For instance, we can assume that there exists an unknown kind of matter with uniform density and uniform negative pressure, dubbed dark energy; the cosmological constant is the simplest realization of this scheme. Alternatively, we can propose a modified theory of gravitation, which, however, must have observational consequences for the Solar System experiments coinciding with those of GR (in error margins), and in cosmological orders of magnitude it must allow descriptions of newly observed phenomena. A recent review of these and other proposals is given by Tsujikawa [7].

In the present paper we concentrate on investigations of viability of cosmological models of general scalar-tensor theories of gravity (STG) which employ a scalar field $\Psi(x)$ besides the usual metric tensor $g_{\mu\nu}(x)$ to describe gravity [8, 9]. In particular, we clarify the relations between GR and STG and indicate that the position of GR in a general STG is singular in many aspects. Nevertheless, the theories must nearly coincide at explaining the Solar System experiments. We mostly review our earlier publications [10–13] and add some extra examples of cosmological evolution in the end.

1. Full equations for cosmological models

General scalar-tensor gravity in the Jordan frame is governed by the action

$$S = \frac{1}{2\kappa^2}\int d^4x\sqrt{-g}\left[\Psi R(g) - \frac{\omega(\Psi)}{\Psi}\nabla^\rho\Psi\nabla_\rho\Psi - 2\kappa^2 V(\Psi)\right] + S_m. \tag{1}$$

Here $\omega(\Psi)$ is a coupling function (we assume that $2\omega(\Psi)+3 \geq 0$ to avoid ghosts in the Einstein frame, see e.g. [14]) and $V(\Psi) \geq 0$ is a potential, ∇_μ denotes the covariant derivative with respect to the metric $g_{\mu\nu}$, S_m is the matter action, and κ^2 is the non-variable part of the effective gravitational constant $\frac{\kappa^2}{\Psi}$. In order to keep the latter positive we assume that $0 < \Psi < \infty$.

The field equations for the flat FLRW line element

$$ds^2 = -dt^2 + a(t)^2\left(dr^2 + r^2(d\theta^2 + \sin^2\theta d\varphi^2)\right) \tag{2}$$

and barotropic fluid ($p = \mathrm{w}\rho,\ \mathrm{w} = \mathrm{const}$) read

$$H^2 = -H\frac{\dot\Psi}{\Psi} + \frac{1}{6}\frac{\dot\Psi^2}{\Psi^2}\,\omega(\Psi) + \frac{\kappa^2}{\Psi}\frac{\rho}{3} + \frac{\kappa^2}{\Psi}\frac{V(\Psi)}{3}, \tag{3}$$

$$2\dot H + 3H^2 = -2H\frac{\dot\Psi}{\Psi} - \frac{1}{2}\frac{\dot\Psi^2}{\Psi^2}\,\omega(\Psi) - \frac{\ddot\Psi}{\Psi} - \frac{\kappa^2}{\Psi}\mathrm{w}\rho + \frac{\kappa^2}{\Psi}\,V(\Psi), \tag{4}$$

$$\ddot\Psi = -3H\dot\Psi - \frac{1}{2\omega(\Psi)+3}\,\frac{d\omega(\Psi)}{d\Psi}\,\dot\Psi^2 + \frac{\kappa^2}{2\omega(\Psi)+3}(1-3\mathrm{w})\rho + \\ + \frac{2\kappa^2}{2\omega(\Psi)+3}\left[2V(\Psi) - \Psi\,\frac{dV(\Psi)}{d\Psi}\right], \tag{5}$$

where $H \equiv \dot a/a$. Upon introducing the notation

$$A(\Psi) \equiv \frac{d}{d\Psi}\left(\frac{1}{2\omega(\Psi)+3}\right), \quad W(\Psi) \equiv 2\kappa^2\left(2V(\Psi) - \frac{dV(\Psi)}{d\Psi}\Psi\right) \tag{6}$$

and substituting H from Eq. (3) in Eq. (5), we get

$$\ddot{\Psi} = \left(\frac{3}{2\Psi} + \frac{1}{2}A(\Psi)(2\omega(\Psi)+3)\right)\dot{\Psi}^2 + \frac{\kappa^2}{2\omega(\Psi)+3}(1-3\mathrm{w})\rho \pm \\ \pm \frac{1}{2\Psi}\sqrt{3(2\omega(\Psi)+3)\dot{\Psi}^2 + 12\kappa^2\Psi(V(\Psi)+\rho)}\,\dot{\Psi} + \frac{W(\Psi)}{2\omega(\Psi)+3}. \tag{7}$$

In the limit $\frac{1}{(2\omega(\Psi)+3)} \to 0$, $\dot{\Psi} \neq 0$ the system faces a spacetime curvature singularity, since H diverges, and likewise behaves $\ddot{\Psi}$. At first, the limit (a) $\frac{1}{(2\omega(\Psi)+3)} \to 0$, (b) $\dot{\Psi} \to 0$ seems only slightly less mathematically precarious for the equations are left just indeterminate (contain terms $0/0$). Yet the latter situation is of particular physical importance, as the experiments in the Solar System (where matter density dominates over the scalar potential), i.e. the limits of observed values of the parametrized post-Newtonian (PPN) parameters and the time variation of the gravitational constant [1],

$$8\pi G = \frac{\kappa^2}{\Psi}\frac{2\omega+4}{2\omega+3}, \tag{8}$$

$$\beta - 1 \equiv \frac{\kappa^2}{G}\frac{\frac{d\omega}{d\Psi}}{(2\omega+3)^2(2\omega+4)} \lesssim 10^{-4}, \tag{9}$$

$$\gamma - 1 \equiv -\frac{1}{\omega+2} \lesssim 10^{-5}, \tag{10}$$

$$\frac{\dot{G}}{G} \equiv -\dot{\Psi}\frac{2\omega+3}{2\omega+4}\left(G + \frac{2\frac{d\omega}{d\Psi}}{(2\omega+3)^2}\right) \lesssim 10^{-13}\ \mathrm{yr}^{-1}, \tag{11}$$

suggest the present cosmological background value of the scalar field to be very close to the limit (a)–(b). Since in this limit the STG PPN parameters coincide with those of general relativity, we may tentatively call (a)–(b) “the limit of general relativity” or “GR point”.

Let us define $\Psi_\star$ by $\frac{1}{2\omega(\Psi_\star)+3} = 0$. In our previous papers [10–13] we studied the limit (a)–(b) with the simplifying assumptions (c) $A_\star \equiv A(\Psi_\star) \neq 0$ and (d) $\frac{1}{2\omega+3}$ is differentiable at $\Psi_\star$, which enabled to Taylor expand the functions in Eq. (7) and find analytic solutions in the phase space for the resulting approximate equation. The outcome was that the solutions are well behaved in this limit, motivating the inclusion of $(\Psi = \Psi_\star,\ \dot{\Psi} = \dot{\Psi}_\star \equiv 0)$ as a boundary point to the open domain of definition of Eq. (7). Moreover, it was possible to identify a wide class of STGs where the FLRW cosmological dynamics spontaneously draws the scalar field to this limit, i.e. into agreement with current local weak field observations in the Solar System.

In what follows, we will consider the era when the cosmological energy density of the scalar potential dominates over the energy density of ordinary matter, i.e. we can take $\rho = 0$ which is a considerable simplification.

2. Approximate equations

Equation (7) with $\rho = 0$ cannot be integrated without specifying the two arbitrary functions $\omega(\Psi)$ and $V(\Psi)$. But being interested in the behaviour of solutions close to the GR point $(\Psi_\star,\ \dot{\Psi}_\star)$ we can still proceed by considering an approximation which maintains the key properties of the full system near this point. We also assume that additional conditions (a)–(d) hold; although these assumptions somewhat constrain the possible forms of ω, we are still dealing with a wide and relevant class of theories.

Let us focus around the point in the phase space, which corresponds to the limit of GR, $\Psi = \Psi_\star + x$, $\dot{\Psi} = \dot{\Psi}_\star + y = y$, where x and y span the neighbourhood of first order small distance from $(\Psi_\star,\ \dot{\Psi}_\star)$. As phase space variables x and y are independent from each other, their ratio y/x is indeterminate at $(x = 0,\ y = 0)$. The meaning of this indeterminacy is perhaps better illuminated in the polar coordinates (ρ, θ), where the radius ρ is a first order small quantity, but $y/x \equiv \tan\theta \in (-\infty, \infty)$ becomes infinitely multivalued at the origin.

We can Taylor expand

$$\frac{1}{2\omega(\Psi)+3} = \frac{1}{2\omega(\Psi_\star)+3} + A_\star x + \cdots \approx A_\star x. \tag{12}$$

Let us denote the values of some functions at $(\Psi_\star,\ \dot{\Psi}_\star)$ as

$$C_1 \equiv \pm\sqrt{\frac{3\kappa^2 V(\Psi_\star)}{\Psi_\star}}, \quad C_2 \equiv A_\star W_\star, \tag{13}$$

where $W_\star \equiv W(\Psi_\star)$ and $V(\Psi_\star) \geq 0$. The three constants $A_\star$, $W_\star$, C_1 determine the leading terms in expansions of the two functions $\omega(\Psi)$, $V(\Psi)$ which specify a STG. Now the expansion of the solution for H of the Friedmann constraint (3) reads

$$H = \frac{C_1}{3} - \frac{1}{2\Psi_\star}\dot{x} + \frac{1}{2C_1\Psi_\star}\left(\frac{C_1^2}{3} - \frac{C_2}{2A_\star\Psi_\star}\right)x + \frac{1}{8C_1\Psi_\star A_\star}\,\frac{\dot{x}^2}{x} + \cdots \tag{14}$$

This explains the introduction of the $\pm$ sign in the definition of C_1 in Eq. (13), as near the GR point $(x = 0,\ y = 0)$ a positive constant, $C_1 > 0$, describes an expanding de Sitter Universe, while a negative one, $C_1 < 0$, describes a contracting de Sitter Universe. An expansion of the effective barotropic index which determines the behaviour of dark energy reads

$$\mathrm{w}_{\text{eff}} \equiv -1 - \frac{2\dot{H}}{3H^2} = -1 + \frac{1}{C_1^2\Psi_\star}\left[\frac{3}{2}\left(1 + \frac{1}{\Psi_\star A_\star}\right)\frac{\dot{x}^2}{x} - 4C_1\dot{x} + 3C_2 x\right] + \cdots \tag{15}$$

A necessary condition for crossing the so-called phantom divide, $\mathrm{w}_{\text{eff}} = -1$, is vanishing of the second term in Eq. (15). This occurs if $\dot{x}$ equals to a solution of the corresponding quadratic equation

$$\dot{x} = \frac{A_\star\Psi_\star}{3(1 + A_\star\Psi_\star)}\left[C_1 \pm \sqrt{D}\right]x \equiv l_\pm x, \quad D \equiv C_1^2 - \frac{9C_2}{8}\left(1 + \frac{1}{A_\star\Psi_\star}\right). \tag{16}$$

Here we can see a condition on the constants $A_\star$, $\Psi_\star$, C_1, C_2 which characterize the theory: $l_\pm$ must be real numbers, i.e. $D \geq 0$. Note that on the plane $(x, \dot{x})$ the phantom divide (16) consists of two straight lines crossing at the origin $x = 0$, $\dot{x} = 0$.

In approximate equations we must recognize the term y^2/x as being the same order as x and y. In other words, we consider all finite values of $\tan\theta$, and exclude only its infinite value on the y-axis which is outside the domain of definition of the system as said before. Thus, keeping the term y^2/x in the approximation of Eq. (7) we obtain a second-order nonlinear differential equation

$$\ddot{x} + C_1\,\dot{x} - C_2\,x = \frac{\dot{x}^2}{2x} \tag{17}$$

and the corresponding first-order system reads

$$\dot{x} = y, \quad \dot{y} = \frac{y^2}{2x} - C_1\, y + C_2\, x. \tag{18}$$

3. Phase trajectories

The phase trajectories for the nonlinear approximate system (18) are determined by the equation

$$\frac{dy}{dx} = \frac{y}{2x} - C_1 + \frac{x}{y}\, C_2. \tag{19}$$

Its solutions

$$|x|K = \left|\frac{1}{2}y^2 + C_1 yx - C_2 x^2\right| \exp(-C_1 f(u)), \quad u \equiv \frac{y}{x}\,, \tag{20}$$

depend on the sign of the expression $C_1^2 + 2C_2 \equiv C$, as the function $f(u)$ is given by

$$f(u) = \begin{cases} \dfrac{1}{\sqrt{C}} \ln\left|\dfrac{u + C_1 - \sqrt{C}}{u + C_1 + \sqrt{C}}\right| & \text{if } \ C > 0, \\ -\dfrac{2}{u + C_1} & \text{if } \ C = 0, \\ \dfrac{2}{\sqrt{|C|}} \left(\arctan \dfrac{u + C_1}{\sqrt{|C|}} + n\pi\right) & \text{if } \ C < 0. \end{cases} \tag{21}$$

Here K is a constant of integration which identifies the trajectory according to initial data $(x_0\,,\ y_0)$.

In general, the right-hand side of Eq. (19) can be written as a quotient of two second order homogeneous polynomials; a qualitative classification of the solutions of differential equations of this type was given by Lyagina [15] long time ago. In a nutshell, the phase portraits for different values of the constants C_1 and C_2 classify according to the number of sectors which form on the phase space around the origin $(x = 0,\ y = 0)$, and the topology of trajectories which inhabit these sectors. The sectors are separated by the boundary $x = 0$ and invariant directions. The latter are lines $y = kx$ where the constant k is a real solution of an algebraic equation

$$k = \frac{k}{2} - C_1 + \frac{C_2}{k}, \tag{22}$$

i.e straight trajectories $y = (-C_1 \pm \sqrt{C})x$ satisfying (19). All possible options are listed in Table 1 and graphically depicted in Fig. 1.

In our recent paper [12] we have argued in detail, that the phase portraits of the nonlinear approximation display the same basic characteristic features we inferred about the solutions of the full system. First, on the horizontal axis $(y = 0)$ the tangents of the trajectories are vertically aligned if $C_2 \neq 0$, and the direction of the flow across $y = 0$ is determined by the sign of $\left.\dfrac{d^2x}{dy^2}\right|_{y=0}$. If $C_2 = 0$ the horizontal axis is populated by fixed points. Second, next to the vertical axis $(x = 0)$ the trajectories turn vertical and do not cross or intersect with the $x = 0,\ y \neq 0$ line, deemed to be outside of the domain of definition of the system. Inspection of the phase portraits in Fig. 1 at the origin $(x = 0,\ y = 0)$ where the sectors meet shows that in all cases there

Table 1

The topology of trajectories of the nonlinear approximation (19)

	No.	Parameters		Topology of trajectories
$C>0$	1.a	$C_1>0$	$C_2>0$	2 hyperb., 2 st. & 2 unst. parab. sectors
	1.b	$C_1>0$	$C_2=0$	1 stable & 1 unstable parabolic sector, 2 stable sectors of degenerate fixed points
	1.c	$C_1>0$	$-\frac{C_1^2}{2}<C_2<0$	2 elliptic, 4 stable parabolic sectors
	1.d	$C_1=0$	$C_2>0$	2 hyperb., 2 st. & 2 unst. parab. sectors
	1.e	$C_1<0$	$C_2>0$	2 hyperb., 2 st. & 2 unst. parab. sectors
	1.f	$C_1<0$	$C_2=0$	1 stable & 1 unstable parabolic sector, 2 unst. sectors of degenerate fixed points
	1.g	$C_1<0$	$-\frac{C_1^2}{2}<C_2<0$	2 elliptic, 4 unstable parabolic sectors
$C=0$	2.a	$C_1>0$	$C_2=-\frac{C_1^2}{2}$	2 elliptic, 2 stable parabolic sectors
	2.b	$C_1=0$	$C_2=0$	2 stable & 2 unstable parabolic sectors
	2.c	$C_1<0$	$C_2=-\frac{C_1^2}{2}$	2 elliptic, 2 unstable parabolic sectors
$C<0$	3.a	$C_1>0$	$C_2<-\frac{C_1^2}{2}$	2 elliptic sectors
	3.b	$C_1=0$	$C_2<0$	2 elliptic sectors
	3.c	$C_1<0$	$C_2<-\frac{C_1^2}{2}$	2 elliptic sectors

are multiple trajectories (identified by different values of K) which all reach the point in question. The trajectories "bounce back" from the origin, so that y changes its sign along a trajectory in all cases, for there is always a class of trajectories whose tangent is vertically aligned at this point. Despite the fact that there seems to be a loss of predictability here (the initial condition $x_0=0$, $y_0=0$ does not fix the constant K uniquely), it would be natural to continue all such trajectories through this point keeping the same K along them. Finally, those trajectories which reach the origin under finite $\tan\theta$ must either begin or end their flow at this point, like it happens at a regular fixed point.

To summarize the results, it turns out that the GR point is an attractor for the asymptotic flow of all trajectories only if $C_1>0$ and $C_2<0$ (cases 1c, 2a, 3a). If $C_1>0$ and $C_2=0$ all trajectories flow to the line $\Psi\neq\Psi_\star$, $\dot{\Psi}=0$ instead (case 1b). If $C_1=0$ and $C_2<0$ all trajectories loop through the GR point oscillating back and forth (nonlinear case 3b), or if $C_1<0$ and $C_2<-\frac{C_1}{2}$ they oscillate further and further (nonlinear case 3c). For the rest of the values of C_1 and C_2 all trajectories eventually flow away from the GR point.

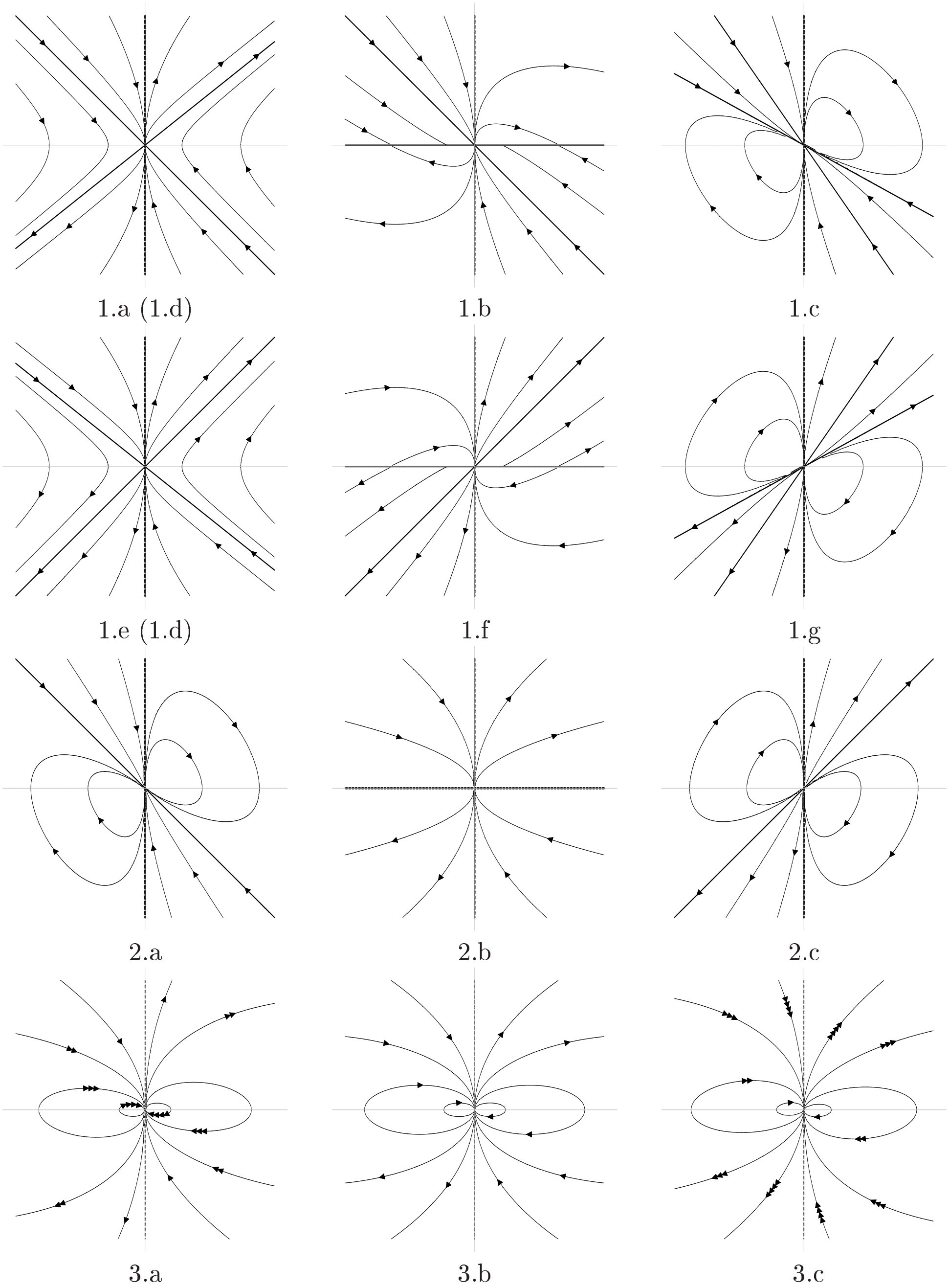

Fig. 1. Phase portraits of the nonlinear approximation (19) near the GR point (Axes: $x = \Psi - \Psi_\star$ horizontal and $y = \dot{\Psi}$ vertical)

4. Solutions

The general solution of Eq. (17) reads

$$\pm x(t) = \exp(-C_1 t)\left[M_1 \exp\left(\frac{1}{2}t\sqrt{C_1^2 + 2C_2}\right) - M_2 \exp\left(-\frac{1}{2}t\sqrt{C_1^2 + 2C_2}\right)\right]^2, \quad (23)$$

where M_1 and M_2 are arbitrary constants of integration. The solutions are classified according to the scheme given in the previous section, here let us focus only on those cases which approach the GR limit asymptotically in time (future).

4.1. Exponential solutions. In the case $C > 0$ solutions read

$$\pm x = \exp(-C_1 t)\left[M_1 \exp\left(\frac{1}{2}t\sqrt{C}\right) - M_2 \exp\left(-\frac{1}{2}t\sqrt{C}\right)\right]^2 . \tag{24}$$

If $C_1 > 0$ and $C_2 < 0$ the solutions exponentially converge to the GR limit, behaving as

$$\pm x|_{t\to\infty} = \exp\left(-(C_1 - \sqrt{C})(t - t_1)\right). \tag{25}$$

Here we have denoted the constant of integration as $M_1 \equiv \exp\left(-\frac{1}{2}t_1(\sqrt{C} - C_1)\right)$ for some arbitrary moment t_1. All solutions satisfy an asymptotic condition

$$\left.\frac{\dot{x}}{x}\right|_{t\to\infty} = \frac{\sqrt{C} - C_1}{\sqrt{C}}. \tag{26}$$

The Hubble parameter reads

$$H|_{t\to\infty} = \frac{C_1}{3} \pm \frac{\exp\left(-(C_1 - \sqrt{C})(t - t_1)\right)}{2\Psi_\star}\left[\frac{C_1 - \sqrt{C}}{2A_\star\Psi_\star} + \frac{4}{3}C_1 - \sqrt{C}\right] \tag{27}$$

and effective barotropic index (15) can be calculated

$$\mathrm{w}_{\mathrm{eff}}|_{t\to\infty} = -1 \pm \frac{\exp\left(-(C_1 - \sqrt{C})(t - t_1)\right)}{C_1^2\Psi_\star} \times \\ \times \left[\frac{3(C_1 - \sqrt{C})^2}{2A_\star\Psi_\star} + 4C_1^2 + 3C - 7C_1\sqrt{C})\right]. \tag{28}$$

Now we can determine whether a model in the theory characterized by distinct parameters ($C_1, C \equiv C_1^2 + 2C_2, A_\star$) approaches the de Sitter spacetime from the quintessence side ($\mathrm{w}_{\mathrm{eff}} > -1$) or from the phantom side ($\mathrm{w}_{\mathrm{eff}} < -1$). Approximate expressions of the PPN parameters (9), (10) indicate that they approach the GR values $\beta = 1$, $\gamma = 1$ exponentially.

Solutions (24) may have interesting features at certain finite moments of time. Firstly, if the theory allows phantom divide, i.e. if $l_\pm$ in Eq. (16) are real numbers, then solutions (24) may cross the phantom divide no more than at two moments $t_\pm$. Secondly, at finite moments t_b some solutions can achieve $x(t_b) = 0$, $\dot{x}(t_b) = 0$ depending on values of integration constants M_1, M_2. Phase trajectories have a vertical slope there and can be described as "turning back" if we consider solutions (24) with only one sign ($+$ or $-$).

4.2. Linear exponential solutions. In the case $C = 0$ the solutions read

$$\pm x = \exp(-C_1 t)\left[\exp\left(\frac{1}{2}C_1 t_1 t\right) - M_2\right]^2 \tag{29}$$

with $M_1 \equiv \exp\left(\frac{1}{2}C_1 t_1\right)$. If $C_1 > 0$ the solutions exponentially converge to the GR limit, behaving as

$$\pm x|_{t\to\infty} = t^2 \exp\left(-C_1(t - t_1)\right). \tag{30}$$

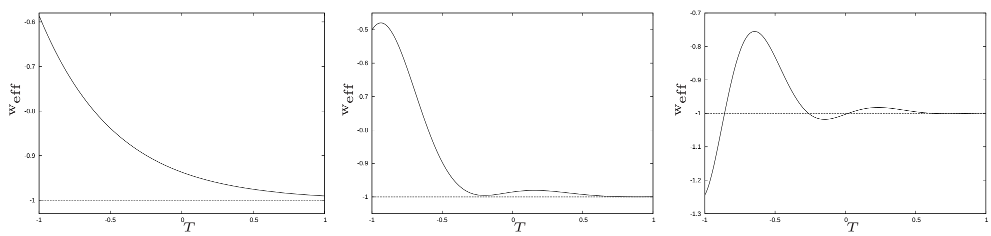

Fig. 2. Examples of the time evolution of w_{eff} for different STG models: (32) left, (33) middle, (34) right

This case is rather finetuned by the condition $C_1^2 = -2C_2$.

4.3. Oscillating solutions. In the case $C < 0$ the solutions read

$$\pm x = \exp\left(-C_1 t\right) \left[N_1 \sin\left(\frac{1}{2} t \sqrt{|C|}\right) - N_2 \cos\left(\frac{1}{2} t \sqrt{|C|}\right) \right]^2 , \tag{31}$$

where N_1, N_2 are integration constants. In terms of the phase space $(x, \dot{x})$, solutions do not have a definite slope at approaching asymptotically ($t \to \infty$) to $x = 0$, $\dot{x} = 0$. As they spiral to it at $t \to \infty$ their phase trajectories cross this point infinitely many times. The spiral, however, must lie in one half-plane of domain of definition, either $x > 0$ or $x < 0$. Approximate expressions of the PPN parameters (9), (10) now reveal damped oscillatory behaviour around the GR values.

If the theory allows crossing the phantom divide, i.e. if $l_\pm$ in Eq. (16) are real, then the possible moments $t_{\pm n}$ of crossing occur on each winding of the spiral. If $l_\pm$ is imaginary, then the effective barotropic index w_{eff} stays below or above -1.

5. Some physical considerations

In order to successfully meet the various observational constraints, the STG scalar field must reside close to the GR point. This occurs naturally when the GR point functions as an attractor for solutions. Therefore, we have a selection principle: only such STG theories are viable and worth further consideration, which possess at least one attractive GR point. Our results [10–13] allow one to immediately decide whether any STG with particular $\omega(\Psi)$ and $V(\Psi)$ is viable or not.

For the evolution of the universe in scalar-tensor cosmology we may envisage a realistic scenario where during the matter domination era the scalar field has already dynamically relaxed sufficiently close to the GR limit [11]. Later when the cosmological energy density of the potential becomes more significant, the solutions given here can be taken to provide a rough description. The final asymptotic state will be de Sitter, but before that we may witness dark energy with variable w_{eff}. Depending on the model, exponential solutions may cross the phantom divide line at most twice before approaching $w_{\mathrm{eff}} = -1$ from either above or below. In the oscillating type of solutions the dark energy effective barotropic index oscillates either in the quintessence regime ($w_{\mathrm{eff}} > -1$), phantom regime ($w_{\mathrm{eff}} < -1$), or crossing the phantom divide line once or twice during each period.

As an illustration, Fig. 2 depicts the dynamics of $w_{\mathrm{eff}} = -1$ for three example solutions in different STG models:

$$\omega(\Psi) = \frac{3\Psi}{2(1-\Psi)}, \quad \kappa^2 V(\Psi) = \frac{2}{3}\left[1 + (1-\Psi)^2\right], \tag{32}$$

$$\omega(\Psi) = \frac{5\Psi}{7(1-\Psi)}, \quad \kappa^2 V(\Psi) = 3\exp\left[3(1-\Psi)\right[, \tag{33}$$

$$\omega(\Psi) = \frac{\Psi}{2(1-\Psi)}, \quad \kappa^2 V(\Psi) = 3\exp\left[3(1-\Psi)\right]. \tag{34}$$

The first model belongs to class 1c and the sample solution shows a monotonic quintessence type convergence towards de Sitter. The second model belongs to class 3a and is characterized by damped oscillations in the quintessence regime. The third model also belongs to class 3.a but exhibits oscillations through the phantom divide line. The initial conditions of these solutions have been chosen such that the corresponding PPN parameters are within observationally allowed limits. The evolution is measured in the units of the analogue of Hubble time, $T = H_\star t = \dfrac{C_1}{3} t$. We may notice that it is possible to have the period of oscillations to be about the same order of magnitude as the age of the Universe.

Research is supported by the Estonian Science Foundation Grant No. 7185 and by Estonian Ministry for Education and Science Support Grant No. SF0180013s07. M.S. also acknowledges the Estonian Science Foundation Postdoctoral research Grant No. JD131.

Резюме

Л. Ярв, П. Кууск, М. Саал. Скалярно-тензорные космологии с потенциалом в пределе общей теории относительности.

Рассматриваются космологические модели фридмановского ($k = 0$) типа в рамках скалярно-тензорных теорий гравитации в представлении Йордана с двумя произвольными функциональными степенями свободы. Предлагается нелинейное приближенное уравнение скалярного поля для описания эпохи, когда плотность энергии скалярного потенциала значительно превышает энергию обычной материи, и модель мало отличается от соответствующей модели общей теории относительности. Рассматривается фазовое пространство скалярного поля, и приводится полная классификация возможных фазовых портретов, а также решения уравнения скалярного поля в космологическом времени в особенности для моделей, асимптотически близких соответствующим моделям общей теории относительности. Показано, что решения могут характеризоваться как экспоненциальным стремлением к соответствующим решениям в общей теории относительности, так и затухающими колебаниями вокруг них.

Ключевые слова: скалярно-тензорные космологии, предел общей теории относительности, темная энергия.

References

1. *Will C.M.* The confrontation between the general relativity and experiment // Living Rev. Rel. – 2005. – V. 9, No 3. – URL: http://www.livingreviews.org/lrr-2006-3.

2. *Jain B., Khoury J.* Cosmological Tests of Gravity // Ann. Phys. – 2010. – V. 325, No 7. – P. 1479–1516.

3. *Lidsey J.E., Wands D., Copeland E.J.* Superstring Cosmology // Phys. Repts. – 2000. – V. 337. – P. 343–492.

4. *Misner C.W., Thorne K.S., Wheeler J.A.* Gravitation. – San Francisco: W. H. Freeman and Co., 1973. – XXVI + 1279 p.

5. *Perlmutter S. et al.* (*Supernova Cosmology Project Collaboration*) Measurements of Ω and Λ from 42 high-redshift supernovae // Astrophys. J. – 1999. – V. 517, No 2. – P. 565–586.

6. *Riess A. G. et al. (Supernova Search Team Collaboration)* Observational evidence from supernovae for an accelerating Universe and a cosmological constant // Astronom. J. – 1998. – V. 116, No 3. – P. 1009–1038.

7. *Tsujikawa S.* Dark energy: investigation and modeling. – arXiv:1004.1493v1 [astro-ph.CO]. – 2010. – 49 p. – URL: http://arxiv.org/pdf/1004.1493v1.pdf.

8. *Faraoni V.* Cosmology in Scalar-Tensor Gravity. – Dordrecht: Kluwer Acad. Publ., 2004. – XIII + 267 p.

9. *Fujii Y., Maeda K.* The Scalar-Tensor Theory of Gravitation. – Cambridge: Cambridge Univ. Press, 2003. – XIV + 246 p.

10. *Järv L., Kuusk P., Saal M.* Scalar-tensor cosmology at the general relativity limit: Jordan vs Einstein frame // Phys. Rev. D. – 2007. – V. 76, No 10. – P. 103506-1–103506-9.

11. *Järv L., Kuusk P., Saal M.* Scalar-tensor cosmologies: fixed points of the Jordan frame scalar field // Phys. Rev. D. – 2008. – V. 78, No 8. – P. 083530-1–083530-11.

12. *Järv L., Kuusk P., Saal M.* Scalar-tensor cosmologies with a potential in the general relativity limit: phase space view // Phys. Rev. D. – 2010. – V. 81, No 10. – P. 104007-1–104007-10.

13. *Järv L., Kuusk P., Saal M.* Scalar-tensor cosmologies with a potential in the general relativity limit: time evolution // Phys. Lett. B. – 2010. – V. 694, No 1. – P. 1–5.

14. *Esposito-Farese G., Polarski D.* Scalar-tensor gravity in an accelerating universe // Phys. Rev. D. – 2001. – V. 63, No 6. – P. 063504-1–063504-20.

15. *Lyagina L.S.* Integral'nye krivye uravneniya $y' = \dfrac{ax^2+bxy+cy^2}{dx^2+exy+fy^2}$ // Uspekhi Mat. Nauk. – 1951. – V. 6, No 2(42). – P. 171–183.

Поступила в редакцию
10.12.10

Järv, Laur – PhD, Senior Research Fellow, Institute of Physics, University of Tartu, Estonia.

Ярв, Лаур Якович – кандидат наук, старший научный сотрудник Института физики Тартуского университета, г. Тарту, Эстония.

E-mail: *laur@fi.tartu.ee*

Kuusk, Piret – Doctor of Physics and Mathematics, Head of the Laboratory of Theoretical Physics, Institute of Physics, University of Tartu, Estonia.

Кууск, Пирет Харальдовна – доктор физико-математических наук, заведующий лабораторией теоретической физики Института физики Тартуского университета, г. Тарту, Эстония.

E-mail: *piret@fi.tartu.ee*

Saal, Margus – PhD, Postdoctoral Fellow, Tartu Observatory, Estonia.

Саал, Маргус Энделович – кандидат наук, научный сотрудник Тартуской обсерватории, г. Тарту, Эстония.

E-mail: *margus@fi.tartu.ee*